IEEE Access
Multidisciplinary | Rapid Review | Open Access Journal

Received November 14, 2019, accepted December 2, 2019, date of publication December 10, 2019,
date of current version December 23, 2019.

Digital Object Identifier 10.1109/ACCESS.2019.2958855

Filtered Extended State Observer Based Line-of-Sight Guidance for Path Following of Unmanned Surface Vehicles With Unknown Dynamics and Disturbances

MINGCONG LI[1], CHEN GUO[2], (Member, IEEE), AND HAOMIAO YU[3]
[1]Marine Electrical Engineering College, Dalian Maritime University, Dalian 116026, China
[2]Institute of Ship Automation and Simulator, Marine Electrical Engineering College, Dalian Maritime University, Dalian 116026, China
[3]Marine Electrical Engineering College, Dalian Maritime University, Dalian 116026, China

Corresponding author: Chen Guo (dmuguoc@126.com)

This work was supported in part by the National Natural Science Foundation of China under 51579024, Grant 83115032, Grant 51879027, and Grant 51809028, and in part by the Fundamental Research Funds for the Central Universities under Grant DMU 3132016311, Grant 3132019109, and Grant 3132019318.

ABSTRACT This paper investigates the path following problem for an underactuated unmanned surface vehicle (USV) in the presence of ocean currents, model uncertainties and input saturation. Firstly, a novel filtered extended state observer (FESO) based line-of-sight (LOS) guidance law is proposed. The FESO is employed to estimate the time-varying sideslip angle caused by ocean, wind and wave disturbances, which is incorporated into the proposed LOS guidance scheme. Then the path following control system is developed to keep the USV moving on the desired path by combining adaptive fuzzy technique with sliding mode method, where adaptive fuzzy technique is applied to deal with model uncertainties. Besides, an auxiliary system is designed to solve the issue of actuator saturation. By using Lyapunov's stability theory, the closed-loop system is shown to be semiglobally uniformly ultimately bounded (SGUUB). Lastly, the comparison simulation results demonstrate the correctness and effectiveness of the proposed scheme.

INDEX TERMS Unmanned surface vehicle, filtered extended state observer, line-of-sight, path following, adaptive fuzzy technique.

I. INTRODUCTION

Over the last few decades, motion control of USV has become a popular research area on both civilian and military fields, including path following, trajectory tracking, dynamic positioning, *etc*. [1]–[5], and the path following problem has been extensively researched. Actually, path following is such a difficult part of USV motion control due to its kinematics and dynamics model, besides, the internal and external uncertainties could enhance the difficulty of research.

For path following applications in level surface, the control objective is to keep USV follow a desired path without time information. A frequently used and effective way to attain convergence to the desired path is to implement a look-ahead LOS guidance law imitating a seasoned sailor [6], and the LOS guidance law has been applied diffusely in path following control system designs [7]–[11]. A traditional straight-line LOS guidance law for path following is proposed in [5], but the sideslip angle caused by external interference is not taken into account. Note that the sideslip angle would magnify the tracking errors and even lead to the instability of the cascade system. To compensate for the sideslip angle, the most direct way is to measure it by instruments, such as GPS, accelerometers and other sensors [12]. However, the noise and high cost of the sensors make this approach impractical. To solve the problem of sensors, a feasible scheme with the purpose of reducing the impact of sideslip angle is the integral LOS (ILOS) guidance [8], which is done only by adding an integral term into the traditional LOS algorithm. Then Fossen proposed an adaptive sideslip LOS (ALOS) guidance law [1], in which the sideslip angle is estimated by the adaptive law. At the same time, the system stability was proved to be achievable for a class of proportional LOS guidance laws used for USV path

The associate editor coordinating the review of this manuscript and approving it for publication was Juntao Fei.

following control. The ALOS algorithm mentioned above is actually a special case of ILOS with a constant sideslip angle. Both the ILOS and ALOS scheme can only manage time-invariant sideslip angle, whereas the sideslip angle is always time-varying in practice due to the external disturbances or when USV tracking a curved path. In this context, an extended state observer (ESO) and a predictor nested into LOS guidance law were proposed by Liu [13], [14] thereby leading to the ESO-based LOS (ELOS) and predictor based-LOS (PLOS) schemes, whereby the estimation of sideslip angle was derived from ESO and predictor, respectively. However, the sideslip angle needs to be limited to a small range. From this point, a finite-time sideslip observer was developed by Wang [15], [16], which can calculate any magnitude sideslip angle accurately in a finite time. It should be pointed out that the differential explosion will occur in the estimation error of the observer in [13]–[16]. Therefore, it an LOS guidance law that can estimate the time-varying sideslip angle without differential explosion.

In addition to guidance, the complete path following system should also contain the execution system, that is, design control system to make the USV velocity and attitude meet the requirements of LOS guidance. Trajectory linearization was first applied in USV path following control field by Qiu [17], [18]. In [19], the controller combining LOS guidance law with active-disturbance-rejection controller is designed to maneuver the USV to follow a desired parameterized path. A global finite-time control system based on backstepping sliding mode control technique was proposed by Yi *et al.* [20], whereby the following errors converge to fixed bounds in a finite time. Skjetne and Fossen [21] proposed a path following controller based on the linearization of the dynamic model and kinematics model transformation in Serret-Frenet coordinate. Based on [21], Do [22] designed an output feedback control law and proved that the control law can guarantee the convergence of USV. However, the aforementioned controllers cannot deal with the disturbances caused by external environment. Using the backstepping sliding mode technique, nonlinear tracking controllers can be derived in [23] and [24], whereby the upper bounds of external disturbances were estimated by the adaptive method. In [25], a robust adaptive technique was integrated in the decentralized chattering free sliding control design to handle unknown bounded disturbances. However, the sign function in sliding mode control will result in chattering, and the actuator is not allowed to occur such circumstance in reality. There are numerous approaches to prevent it from happening, such as replacing sign function to continues sigmoid function [26], adding filter [27], approximating sign function with fuzzy/neural network [28], constructing the optimization method of sliding switching surface [29], *etc*.

Regarding the nonparametric uncertainties in control systems, the emergence of fuzzy/neural network can solve these problems, these approaches [16], [30]–[32] have been successfully applied to estimate uncertainties and unmodeled dynamics within the control system of USV. In the foregoing discussion, a prominent disadvantage of fuzzy/neural network-based control methods is that the approximators completely lie on the amount of network nodes. The parameters to be designed will grow with the increasing nodes. Concerning the question mentioned above, an alternative approach is using adaptive law to estimate weights [31]–[33]. Regarding the physical properties of the actuator itself, the input saturation caused by physical constraint condition should be taken into account, and it can impact the stability of the whole system distinctly, such as overshoot, oscillate, *etc*. An auxiliary system was designed to compensate for the actuator saturation of USV in some studies [34]–[36] to solve this problem properly.

Motivated by above considerations, a novel FESO-based LOS adaptive fuzzy sliding mode control scheme with input saturation is presented to accomplish straight and curved path following of USV with time-varying sideslip and model uncertainties. The FESO is designed to estimate the time-varying sideslip angles of USV. Meanwhile, the sliding mode controller is to make the actual resultant velocity and the heading angle accurately track the desired signals generated by the FELOS guidance law. The adaptive fuzzy control system is served to estimate model uncertainties.

The rest of the paper is organized as follows. Section 2 gives some preliminaries and problem formulation. Section 3 provides the guidance law design with FESO estimating the time-varying sideslip angles. Section 4 provides the control algorithms of USV. The analysis of the closed-loop system stability is given in Section 5. Some numerical simulations are presented in Section 6 to demonstrate the effectiveness of the proposed scheme. Section 7 concludes the paper.

II. PRELIMINARIES AND PROBLEM FORMULATION

A. PRELIMINARIES

Notation: Throughout this paper, $|\bullet|$ denotes the absolute value of a scalar. $(\bullet)^T$ represents the transpose of a matrix $(\bullet)$. $(\hat{\bullet})$ and $(\tilde{\bullet})$ describe the estimated value and the error of approximation, respectively. $(\bullet)_{\max}$ denotes the maximum value.

To facilitate the FELOS-based path following control scheme design and analysis, some definitions and lemmas are derived.

Definition 1 [37]: x is the solution of the system differential equation. The system $\dot{x} = f(t, x)$ is said to be uniformly ultimately bounded (UUB) if there exists a non-negative constant $T(x_0, W) < \infty$ and an arbitrary constant δ, it satisfies

$$||x(t_0)|| \leq \delta, \quad \forall t \geq t_0 + T \tag{1}$$

The system is globally uniformly ultimately bounded (GUUB) if x radially unbounded.

Lemma 1 [38]: For every $(x, y) \in \mathbb{R}^2$, the Young's inequality can be expressed as

$$xy \leq \frac{\varepsilon^m}{m}|x|^m + \frac{1}{q\varepsilon^q}|y|^q \tag{2}$$

where ε is positive, $p > 1, q > 1$, the condition $(p-1)(q-1) = 1$ must be satisfied.

Lemma 2 [39]: The control input τ_i $(i = u, r)$ of USV are limited by physical constraint and it satisfied $-\tau_{i\max} \leq \tau_i \leq \tau_{i\max}$, so τ_i is defined by the following function of the command τ_{i0},

$$\tau_i = \begin{cases} \tau_{i\max}, & \tau_{i0} > \tau_{i\max} \\ \tau_{i0}, & -\tau_{i\max} \leq \tau_{i0} \leq \tau_{i\max} \\ -\tau_{i\max}, & \tau_{i0} < -\tau_{i\max} \end{cases} \tag{3}$$

Lemma 3 [40]: From *Definition 1*, considering the actual situation, if some uncertainties or disturbances are directly contained the system $\dot{x} = f(t, x)$, f satisfy Lipschitz in x, there exists a smooth function V that is positive definite and radially unbounded such that

$$\dot{V} = \frac{\partial V}{\partial x} f(x, t) \leq -KV + \xi \leq 0, \quad \forall t \geq 0, \ \forall x \in r^n \tag{4}$$

where K is a positive constant and ξ is bounded. Then the system is UUB. If x only exist in a suitable compact Ω, the system is semi-globally uniformly ultimately bounded (SGUUB).

B. PROBLEM FORMULATION

This section describes the 3 degrees-of-freedom (DOF) USV kinematics and dynamics model considering ocean currents. According to [5], the model of USV can be represented by

$$\begin{cases} \dot{x} = u\cos(\psi) - v\sin(\psi) \\ \dot{y} = u\sin(\psi) + v\cos(\psi) \\ \dot{\psi} = r \\ \dot{u} = -\dfrac{d_{11} + d_{11}^q u}{m_{11}} u + \dfrac{(m_{22}v + m_{23}r)}{m_{11}} r \\ \qquad + \boldsymbol{\vartheta}_u^T(\psi, r)\boldsymbol{V}_{xy} + \tau_u + d_u \\ \dot{v} = A(u_r, u_c)r + B(u_r)v_r + d_v \\ \dot{r} = C_r(u, v, r) + \boldsymbol{\vartheta}_r^T(u, v, r, \psi)\boldsymbol{V}_{xy} + \tau_r + d_r \end{cases} \tag{5}$$

where (x, y) describe the position of USV and ψ denotes the orientation in the inertial frame. (u, v, r) refer to the surge, sway velocities and the yaw rate respect to the body-fixed frame, respectively. The terms d_{ij} and d_{ij}^q are hydrodynamic damping in the 3 velocities, and m_{ij} is the rigid-body mass and $m_{ij} \triangleq m_{ij}^{RB} + m_{ij}^A$, where m_{ij}^{RB} denotes the added mass and m_{ij}^A is the inertia mass of USV. $\boldsymbol{V}_{xy} = [V_x, V_y, V_x^2, V_y^2, V_xV_y]^T$, where V_x and V_y refer to the ocean current velocities in the inertial frame. $[u_r, v_r, r]^T = [u, v, r]^T - [u_c, v_c, 0]^T$, where (u_c, v_c) are the ocean current velocities and (u_r, v_r) are the relative velocities between USV and ocean currents within the body-fixed frame. The control input are described as (τ_u, τ_r), and they are called the surge force and yaw moment. The USV is underactuated because there is not input signal of the sway direction. (d_u, d_v, d_r) represent the disturbances caused by external environment without ocean currents, such as wind and waves. The expressions for $\boldsymbol{\vartheta}_u^T(\psi, r)$, $\boldsymbol{\vartheta}_r^T(u, v, r, \psi)$, $A(u_r, u_c)$, $B(u_r)$ and $C_r(u, v, r)$ are shown in Appendix. In addition, considering the external disturbance, the dynamical model of USV is hard to establish accurately, and the USV parameters are always time-varying on the voyage. Therefore, there always exit model uncertainties.

Assumption 1: The ocean currents (V_x, V_y) is constant and bounded within the inertial frame, and they are much less than the surge and sway velocities of USV. In addition, the upper bounds of (d_u, d_v, d_r) are (k_1, k_2, k_3) and they are unknown.

Assumption 2: Define U represents the resultant velocity of USV which is assumed to be bounded and $U = \sqrt{u^2 + v^2}$, U and r are measurable, but (u, v) are unmeasurable.

Remark 1: As is shown in [5] that USV can be described by the 3-DOF kinetic mode and the ocean current is constant in the inertial frame. As for Assumption 2, U, r and ψ can be readily measured by GPS or other navigational instruments. The vector (u, v) can also be measured by using optical correlation sensors but these devices are very expensive, thus making this option difficult to realize [41].

C. CONTROL OBJECTIVE

The control objective is to develop a guidance law ψ_d and control law (τ_u, τ_r) for USV to converges and follows a reference path described by $(x_p(\omega), y_p(\omega))$ with unknown time-varying sideslip angle, in other words, it can be formalized as $\lim_{t\to\infty}(x - x_p) \leq \kappa_x$, $\lim_{t\to\infty}(y - y_p) \leq \kappa_y$, $\lim_{t\to\infty}(u - u_d) \leq \kappa_u$, where u_d is the desired surge velocity and $\kappa_x, \kappa_y, \kappa_u$ are small positive constants.

III. FESO-BASED LOS GUIDANCE LAW

In this section, we describe the geometry of path following and develop FELOS guidance law to calculate the desired heading angle of USV.

A. SIDESLIP ANGLE IDENTIFICATION

The geometrical illustration of LOS is expressed in Fig. 1.

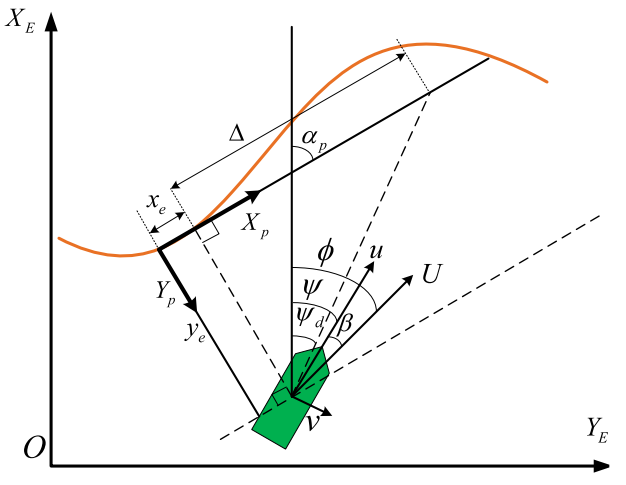

FIGURE 1. LOS guidance geometry.

Consider ω to be the independent variable of reference path $(x_p(\omega), y_p(\omega))$ and $\alpha_p(\omega) = atan2(y_p'(\omega), x_p'(\omega))$ represents the path- tangential angle, where $y_p'(\omega) = \partial y_p/\partial\omega$ and

$x'_p(\omega) = \partial x_p/\partial\omega$. $\beta = atan2(v, u) = \phi - \psi$ represents the sideslip angle of USV, where(ψ, ϕ) are the heading angle and course angle, respectively.

Assumption 3: The velocities of USV changes slowly and the sway is small enough to satisfy the following conditions: The unknown sideslip angle β is small as well as slowly time-varying so that it satisfies that $\dot{\beta} = 0$ and $\sin\beta = \beta$, $\cos\beta = 1$. Besides, β is bounded.

For the point (x, y) where USV located, the following errors between (x, y) and the reference point $(x_p(\omega), y_p(\omega))$ can be compendiously written as follows

$$\begin{bmatrix} x_e \\ y_e \end{bmatrix} = \begin{bmatrix} \cos\alpha_p & -\sin\alpha_p \\ \sin\alpha_p & \cos\alpha_p \end{bmatrix}^T \begin{bmatrix} x - x_p(\omega) \\ y - y_p(\omega) \end{bmatrix} \tag{6}$$

where (x_e, y_e) denote the along and cross tracking errors. The design objective is to force the USV to follow the reference path $(x_p(\omega), y_p(\omega))$ so that the time-varying sideslip can be compensated with the guaranteed transient performance. In other words, the target is to attain $x_e, y_e \to 0$ as $t \to \infty$

Similar to (6), we have

$$\begin{bmatrix} \dot{x}_p(\omega) \\ \dot{y}_p(\omega) \end{bmatrix} = \begin{bmatrix} \cos\alpha_p & -\sin\alpha_p \\ \sin\alpha_p & \cos\alpha_p \end{bmatrix} \begin{bmatrix} u_t \\ 0 \end{bmatrix} \tag{7}$$

where u_t is the virtual velocity along the reference path and $u_t = \dot{\omega}\sqrt{x'^2_p + y'^2_p}$.

By differentiating x_e with respect to time, it follows that

$$\begin{aligned} \dot{x}_e = {} & \dot{x}\cos\alpha_p + \dot{y}\sin\alpha_p - \dot{x}_p(\omega)\cos\alpha_p - \dot{y}_p(\omega)\sin\alpha_p \\ & + \dot{\alpha}_p \underbrace{[-(x - x_p(\omega))\sin\alpha_p + (y - y_p(\omega))\cos\alpha_p]}_{y_e} \end{aligned} \tag{8}$$

Similarly, time differentiation of y_e gives

$$\begin{aligned} \dot{y}_e = {} & \dot{y}\cos\alpha_p + \dot{x}_p(\omega)\sin\alpha_p - \dot{x}\sin\alpha_p - \dot{y}_p(\omega)\cos\alpha_p \\ & - \dot{\alpha}_p \underbrace{[(x - x_p(\omega))\cos\alpha_p + (y - y_p(\omega))\sin\alpha_p]}_{x_e} \end{aligned} \tag{9}$$

Substituting (5), (7), β and u_t into (8) and (9), we have

$$\begin{cases} \dot{x}_e = U\cos(\psi - \alpha_p + \beta) + \dot{\alpha}_p y_e + u_t \\ \dot{y}_e = U\sin(\psi - \alpha_p + \beta) - \dot{\alpha}_p x_e \end{cases} \tag{10}$$

Note that $\sin\beta = \beta$ and $\cos\beta = 1$, rewrite (10) as

$$\begin{cases} \dot{x}_e = U\cos(\psi - \alpha_p) - U\sin(\psi - \alpha_p)\beta + y_e\dot{\alpha}_p - u_t \\ \dot{y}_e = U\sin(\psi - \alpha_p) + U\cos(\psi - \alpha_p)\beta - x_e\dot{\alpha}_p \end{cases} \tag{11}$$

Remark 2: It is worth noting that the sideslip angle β, which describes the angle between course and heading of USV, is unknown from Assumption 2. It has a strong impact on the control system, and if not appropriately compensated, the results will markedly deviate from the reference path.

To estimate the sideslip angle precisely, according to [42], a new FESO is proposed as

$$\begin{cases} E = \hat{y}_{eq} - y_{eq} \\ \dot{\hat{y}}_{eq} = -\frac{1}{\tau}\hat{y}_{eq} + \frac{1}{\tau}\hat{y}_e - \eta_1 E \\ \dot{\hat{y}}_e = \hat{g} - \eta_2 E + U\sin(\psi - \alpha_p) - \dot{\alpha}_p x_e - \eta_3\tilde{y}_e \\ \dot{\hat{g}} = -\eta_4 fal(E, \varepsilon, \delta) - \eta_5\hat{g} \end{cases} \tag{12}$$

where y_{eq} represents the filtered cross tracking error y_e. $\tilde{y}_e = \hat{y}_e - y_e$ and E are estimate errors. $y_1 = y_{eq} - y_e$ denotes the filtering error and $\dot{y}_{eq} = -\frac{1}{\tau}y_{eq} + \frac{1}{\tau}y_e$. The coefficients $\tau, \eta_1, \eta_2, \eta_3, \eta_4, \eta_5$ are positive constants. $g = U\cos(\psi - \alpha_p)\beta$ and $\hat{g} = U\cos(\psi - \alpha_p)\hat{\beta}$. The $fal(\bullet)$ function is defined as

$$fal(E, \varepsilon, \delta) = \begin{cases} |E|^{\varepsilon} sgn(E), & |E| > \delta \\ E/\delta^{1-\varepsilon}, & else \end{cases} \tag{13}$$

where ε and δ are positive parameters, ε is a constant and $0 < \varepsilon < 1$.

The estimation of the sideslip angle can be calculated as

$$\hat{\beta} = \frac{\hat{g}}{U\cos(\psi_d - \alpha_p)} \tag{14}$$

The unknown sideslip angle β is bounded from Assumption. 3 so as to $g = U\cos(\psi - \alpha_p)\beta$ is also bounded since U denotes the actual velocity which must be bounded and $\cos(\psi - \alpha_p) \in [0, 1]$.

By combining with (11), the results can be written as follows

$$\begin{cases} \dot{E} = -\frac{1}{\tau}\tilde{y}_{eq} + \frac{1}{\tau}\tilde{y}_e - \eta_1 E \\ \dot{\tilde{y}}_e = \tilde{g} - \eta_2 E - \eta_3\tilde{y}_e \\ \dot{\tilde{g}} = -\eta_4 fal(E, \varepsilon, \delta) - \eta_5\hat{g} - \dot{g} \end{cases} \tag{15}$$

Theorem 1: The FESO system (12) is UUB with the state being $\hat{y}_e$, $\hat{y}_{eq}$, and the unknown item being $\hat{g}$.

Proof: Construct the following Lyapunov function

$$V_1 = \frac{1}{2}E^2 + \frac{1}{2}y_1^2 + \frac{1}{2}\tilde{y}_e^2 + \frac{1}{2}\tilde{g}^2 \tag{16}$$

Note that $\dot{g} \approx 0$. Differentiating both sides of (16) along (11)-(15) results in

$$\begin{aligned} \dot{V}_1 = {} & E(-\frac{1}{\tau}E - \eta_1 E + \eta_2 E - \frac{1}{\tau}(y_{eq} - y_e)) \\ & + y_1(-\frac{1}{\tau}y_1 + B) + \tilde{y}_e(-\eta_3\tilde{y}_e + \tilde{g} - \eta_2 E) \\ & + \tilde{g}[-\eta_4 fal(E, \varepsilon, \delta) - \eta_5\hat{g}] \\ = {} & (-\frac{1}{\tau} - \eta_1 + \eta_2)E^2 - \frac{1}{\tau}Ey_1 - \frac{1}{\tau}y_1^2 \\ & + y_1 B - \eta_3\tilde{y}_e^2 + \tilde{y}_e\tilde{g} - \eta_2\tilde{y}_e E \\ & - \frac{1}{2}\eta_5\tilde{g}^2 - \eta_4\tilde{g} fal(E, \varepsilon, \delta) + \frac{1}{2}{g_{\max}}^2 \end{aligned} \tag{17}$$

where $B = -g - U\sin(\psi - \alpha_p) + \dot{\alpha}_p x_e + \frac{1}{2}{g_{\max}}^2$ is a continuous vector function which is bounded since the boundness of g and $U\cos(\psi - \alpha_p)$ have already been analyzed above, $\dot{\alpha}_p$ is bounded due to the smooth desired path and the boundness of x_e will be proved later, thus $B \le B_M$ holds for all $B(t)$. For $|E| > \delta$, $|E|^{\varepsilon} sgn(E) \le E$ if $|E| \ge 1$ and $|E|^{\varepsilon} sgn(E) \le 1$ if $|E| < 1$. We just consider the case that $|E| > \max\{\delta, 1\}$ in this paper for the other cases are simple to stability analysis. Based on the above analysis and according to Lemma 1, we have

$$\begin{aligned} \dot{V}_1 \le {} & -(\frac{1}{\tau} + \eta_1 - \eta_2 - \frac{1}{2}\eta_4 - \frac{1}{2})E^2 - (\frac{1}{\tau} - 1)y_1^2 \\ & - (\eta_3 - \frac{1}{2}\eta_2 - \frac{1}{2})\tilde{y}_e^2 - (\frac{1}{2}\eta_5 - \frac{1}{2}\eta_2 - \frac{1}{2}\eta_4 - \frac{1}{2})\tilde{g}^2 + \frac{1}{2}B_M^2 \\ \le {} & -2\mu_1 V_1 + C_1 \end{aligned} \tag{18}$$

where $\mu = \min\{\frac{1}{\tau} + \eta_1 - \eta_2 - \frac{1}{2}\eta_4 - \frac{1}{2}, \frac{1}{\tau} - 1, \eta_3 - \frac{1}{2}\eta_2 - \frac{1}{2}, \frac{1}{2}\eta_5 - \frac{1}{2}\eta_2 - \frac{1}{2}\eta_4 - \frac{1}{2}\}$, $C_1 = \frac{1}{2}B_M^2$ and design parameters satisfying $\frac{1}{\tau} + \eta_1 - \eta_2 - \frac{1}{2}\eta_4 > \frac{1}{2}$, $\frac{1}{\tau} > 1$, $\eta_3 - \frac{1}{2}\eta_2 > \frac{1}{2}$ and $\eta_5 - \frac{1}{2}\eta_2 - \frac{1}{2}\eta_4 > \frac{1}{2}$. Thus, $\dot{V}_1$ is strictly negative outside the range $\varpi_1 = \{V_1 \leq \frac{C_1}{2\mu_1}\}$ and it follows that

$$V_1 \leq (V_1(0) - \frac{C_1}{2\mu_1})e^{-2\mu_1 t} + \frac{C_1}{2\mu_1} \tag{19}$$

Therefore, all the estimated errors in the FESO subsystem (12) is UUB.

Remark 3: Compared with ALOS algorithm in [1], where y_e is served to update the adaptive law for β, the proposed FESO is able to enhance the transient performance of the system by increasing the parameters η_3 and η_5, as well as by initializing $\tilde{y}_e = 0$. As for ESO algorithm in [13], the presented FESO subsystem in this paper get smoother observations because of introducing the filter. Thus, the effect of FESO is closer to reality.

B. GUIDANCE LAW DESIGN

The guidance law is presented as

$$\psi_d = \alpha_p + \arctan\left(-\frac{y_e}{\Delta} - \hat{\beta}\right) \tag{20}$$

where $\Delta > 0$ is the look-ahead distance.

Remark 4: From (20), we have $\psi_d - \alpha_p = \arctan\left(-\frac{y_e}{\Delta} - \hat{\beta}\right)$, which indicates that $\psi_d - \alpha_p \in (-\pi/2, \pi/2)$. Thus, the denominator of (14) is guaranteed to be nonzero.

In (11), u_t can be regarded as a virtual control input to stabilize x_e, Consequently, u_t is designed as

$$u_t = kx_e + U\cos(\psi_d - \alpha_p) \tag{21}$$

where k is a positive parameter. Then, the update law for the reference path parameter ω is proposed as

$$\dot{\omega} = \frac{u_t}{\sqrt{x'^2_p + y'^2_p}} = \frac{kx_e + U\cos(\psi_d - \alpha_p)}{\sqrt{x'^2_p + y'^2_p}} \tag{22}$$

Remark 5: From (21) we may find that the virtual velocity u_t has obvious imparity to trajectory tracking since it is relate to several variates, such as U, x_e, *etc*. It means that the reference path has a reverse reference to actual path and it can go fast or slow. This greatly simplifies the difficulty of path following and reduces the requirements on the input performance of USV.

Substituting (21) into the first equality of (11), we have

$$\dot{x}_e = -kx_e - U\sin(\psi - \alpha_p)\beta + \dot{\alpha}_p y_e \tag{23}$$

Assumption 4: Similar to [13] and [14], the actual heading angle ψ will totally track ψ_d that calculated by FELOS so that $\psi = \psi_d$.

Noting that

$$\begin{cases} \sin\left(\arctan\left(\frac{y_e - \Delta\hat{\beta}}{\Delta}\right)\right) = -\frac{y_e + \Delta\hat{\beta}}{\sqrt{\Delta^2 + (y_e + \Delta\hat{\beta})^2}} \\ \cos\left(\arctan\left(\frac{y_e - \Delta\hat{\beta}}{\Delta}\right)\right) = \frac{\Delta}{\sqrt{\Delta^2 + (y_e + \Delta\hat{\beta})^2}} \end{cases} \tag{24}$$

The second equality of (11) can be expressed as

$$\dot{y}_e = -\frac{Uy_e}{\sqrt{\Delta^2 + (y_e + \hat{\beta})^2}} - \dot{\alpha}_p x_e - \tilde{g} \tag{25}$$

Theorem 2: Subsystem (11), deemed as a system with the state being tracking errors x_e and y_e, the virtual input being $\tilde{g}$ and β, is stable, all the errors in (11) are UUB by setting parameters appropriately.

Proof: Consider the following Lyapunov function

$$\dot{V}_2 = \frac{1}{2}x_e^2 + \frac{1}{2}y_e^2 \tag{26}$$

Differentiating both sides of (26), it follows that

$$\dot{V}_2 = -kx_e^2 - U\sin(\psi_d - \alpha_p)x_e\beta - \frac{Uy_e^2}{\sqrt{\Delta^2 + (y_e + \hat{\beta})^2}} - y_e\tilde{g} \tag{27}$$

Using the following facts:

$$U\sin(\psi - \alpha_p)x_e\beta \leq Ux_e\beta \leq \frac{U}{2\lambda_1}x_e^2 + \frac{U\lambda_1}{2}\beta^2 \tag{28}$$

$$y_e\tilde{g} \leq \frac{1}{2\lambda_2}y_e^2 + \frac{\lambda_2}{2}\tilde{g}^2 \tag{29}$$

and substituting (28) and (29) into (27), we have

$$\begin{aligned} \dot{V}_2 &\leq -\left(k - \frac{U}{2\lambda_1}\right)x_e^2 - \left(h_{\min} - \frac{1}{2\lambda_2}\right)y_e^2 \\ &\quad + \frac{U\lambda_1}{2}\beta^2 + \frac{\lambda_2}{2}\tilde{g}^2 \\ &\leq -2\mu_2 V_2 + C_2 \end{aligned} \tag{30}$$

where $\mu_2 = \min\{k - \frac{U}{2\lambda_1}, h_{\min} - \frac{1}{2\lambda_2}\}$, $C_2 = \frac{U\lambda_1}{2}\beta^2 + \frac{\lambda_2}{2}\tilde{g}^2$ and $h_{\min} = \frac{U_{\min}}{\sqrt{\Delta_{\max}{}^2 + (y_e + \Delta_{\max}\hat{\beta})^2}}$. We can obtain C_2 is bounded from Theorem 1 and Assumption 3.

Thus, $\dot{V}_2$ is strictly negative outside the range $\varpi_2 = \{V_2 \leq \frac{C_2}{2\mu_2}\}$ if design parameters satisfying $k - \frac{U}{2\lambda_1} > 0, h_{\min} - \frac{1}{2\lambda_2} > 0$ and that gives

$$V_2 \leq (V_2(0) - \frac{C_2}{2\mu_2})e^{-2\mu_2 t} + \frac{C_2}{2\mu_2} \tag{31}$$

it follows that the error subsystem (11) is UUB.

The compensation of the sideslip angle is presented in the case of considering the value of look-ahead distance Δ as time-invariant by many researchers [1], [13]–[16]. In principle, a smaller Δ should be selected when the USV is far from the desired path, and this will make the cross-track error y_e decrease faster; a larger Δ is ought to be chosen when USV is close to the desired path. D. Mu *et al* [4] considered the

time-varying look-ahead distance by using fuzzy rules, but the variation tendency of y_e was not taken into account. In this context, an improved fuzzy algorithm to optimize the value of Δ is proposed, and the system has two input entries: y_e and $\dot{y}_e$, the gain $= \lambda$ is the output entry. The final value of Δ can be written as $\Delta = \Delta_{\min} + \lambda(\Delta_{\max} - \Delta_{\min})$. The fuzzy rules are presented as Table 1.

TABLE 1. Fuzzy rules of Δ.

y_e	$\dot{y}_e$				
	NB	NS	Z	PS	PB
NB	VS	VS	VS	VS	S
NS	S	S	M	B	B
Z	B	VB	VB	VB	B
PS	B	B	M	S	S
PB	S	VS	VS	VS	VS

(1) y_e and $\dot{y}_e$ are normalized to $[-1, 1]$; the data domain of λ is $[0, 1]$.

(2) y_e and $\dot{y}_e$ are equally divided into NB, NS, Z, PS and PB; λ is equally divided into VS, S, M, B and VB.

Remark 6: The proposed FELOS guidance law can be used together with the surge and heading controller, where later is designed by integrating backstepping sliding mode technique with fuzzy logic system. As shown in Fig. 2, the surge and sway velocities can be estimated by the estimates sideslip $\hat{\beta}$. The design of the control system will be demonstrated in the next section.

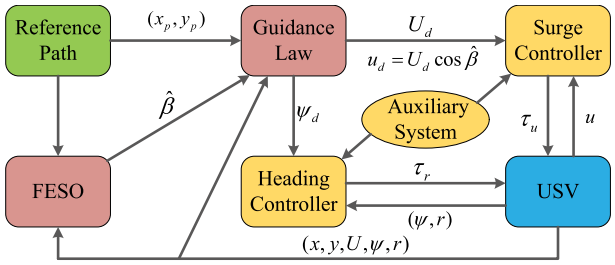

FIGURE 2. The block diagram of the path following scheme.

IV. SURGE AND HEADING CONTROL

A. FUZZY LOGIC SYSTEM

Fuzzy logic system (FLS) can approximate any continuous function and it can be presented as follows

R_j: IF X_1 is F_1^j, X_2 is $F_2^j, \ldots$, and X_n is F_n^j; THEN Y_1 is θ_1^j, Y_2 is $\theta_2^j, \ldots$, and Y_m is θ_m^j, where $X = [X_1, X_2, \ldots, X_n]^T \in \mathbb{R}^n$ and $Y = [Y_1, Y_2, \ldots, Y_m]^T$ are input and output vectors, respectively, where $F_i^j, i = 1, 2, \ldots, n; j = 1, 2, \ldots, N$ is the fuzzy set within *i-th* dimension *j-th* rule and θ_k^j denotes the fuzzy singleton.

The output of FLS is given as follows

$$Y_k = \theta_k^T \xi(X) + \varepsilon, \quad k = 1, 2, \ldots, m \tag{32}$$

where ε is the fuzzy system approximation error, $\theta_k = [\theta_k^1, \theta_k^2, \ldots, \theta_k^N]^T$ and they are bounded by $|\theta_K|| \le \theta_{\max}, \varepsilon \le \varepsilon_{\max}, \xi(X) = [\xi_1(\boldsymbol{X}), \xi_1(\boldsymbol{X}), \ldots, \xi_N(\boldsymbol{X})]^T$ denotes the fuzzy basis function vector expressed as

$$\xi_j(\boldsymbol{X}) = \frac{\prod_{i=1}^n \mu_F^j(X_i)}{\sum_{j=1}^N \prod_{i=1}^n \mu_F^j(X_i)}, \quad j = 1, 2, \ldots, N \tag{33}$$

where $\mu_F^j(X_i)$ is the membership function and is expressed by Gaussian function regularly.

The estimation $\hat{\theta}$ are always applied to approximate the unknown parts of actual systems and then the approximation of Y_K is

$$\hat{Y}_k = \hat{\theta}_k^T \xi(\boldsymbol{X}) \tag{34}$$

We usually define $\tilde{\theta} = \theta - \hat{\theta}$ denotes the estimation error of fuzzy singleton and $\tilde{Y}_K = Y_K - \hat{Y}_K = \tilde{\theta}_K \xi(\boldsymbol{X}) + \varepsilon$ is the system approximation error.

B. CONTROL SYSTEM DESIGN

Define the following variables $u_e = u - u_d$, $s_1 = u_e + c_1 \int_0^t u_e d\tau$, $\psi_e = \psi - \psi_d$ and the sliding surface $s_2 = \dot{\psi}_e + c_2 \psi_e$, where u_d is the desired surge velocity and $u_d = U_d \cos\hat{\beta}$, U_d is the resultant velocity (velocity size). Due to the unmeasurable properties of u,v, define $u = U\cos\hat{\beta}$ and $v = U\sin\hat{\beta}$. The time-derivative of s_1, s_2 and ψ_e can be obtained as

$$\begin{cases} \dot{s}_1 = \underbrace{-\dfrac{d_{11} + d_{11}^q u}{m_{11}} u + \dfrac{(m_{22} v + m_{23} r)}{m_{11}} r}_{g_u} - \dot{u}_d \\ \qquad + \underbrace{\boldsymbol{\vartheta}_u^T(\psi, r)\boldsymbol{V}_{xy}}_{V_u} + \tau_u + d_u + c_1 u_e \\ \dot{s}_2 = c_2 \dot{\psi}_e - \ddot{\psi}_d + \underbrace{\boldsymbol{C}_r(u, v, r)}_{g_r} + \underbrace{\boldsymbol{\vartheta}_r^T(u, v, r, \psi)\boldsymbol{V}_{xy}}_{V_r} \\ \qquad + \tau_r + d_r \\ \dot{\psi}_e = s_2 - c_2 \psi_e \end{cases} \tag{35}$$

By introducing FLS and estimate the unknown dynamic in (35) gives

$$\begin{cases} \hat{g}_u = \hat{\boldsymbol{\theta}}_u^T \boldsymbol{\xi}_1(\boldsymbol{v}) \\ \hat{g}_r = \hat{\boldsymbol{\theta}}_r^T \boldsymbol{\xi}_1(\boldsymbol{v}) \end{cases} \tag{36}$$

In (36), the input of FLS is $\boldsymbol{v}$, where $\boldsymbol{v} = [u, v, r]^T$, the output are $\hat{g}_u$ and $\hat{g}_r$. For the sake of convenience to analyze influence of the input saturation, an auxiliary system is designed as

$$\dot{\chi}_u = \begin{cases} -k_{\chi u}\chi_u - \dfrac{|s_1 \Delta\tau_u + 0.5\Delta\tau_u^2|}{\chi_u^2}\chi_u + \Delta\tau_u, & |\chi_u| \ge \chi_p \\ 0, & |\chi_u| < \chi_p \end{cases} \tag{37}$$

$$\dot{\chi}_r = \begin{cases} -k_{\chi r}\chi_r - \dfrac{|s_2 \Delta\tau_u + 0.5\Delta\tau_r^2|}{\chi_r^2}\chi_r + \Delta\tau_r, & |\chi_r| \ge \chi_p \\ 0, & |\chi_r| < \chi_p \end{cases} \tag{38}$$

where $k_{\chi u}, k_{\chi r}, \kappa_u, \kappa_r$ and χ_p are positive constants. Besides, $\Delta t_u = \tau_u - \tau_{u0}$ and $\Delta t_r = \tau_r - \tau_{r0}$.

The corresponding surge control law and heading control law are designed as follows respectively

$$\begin{cases} \tau_{u0} = -\hat{\boldsymbol{\theta}}_u^T \boldsymbol{\xi}_1(\boldsymbol{v}) + \dot{u}_d - \hat{V}_u - k_1 sgn(s_1) \\ \qquad - c_1 u_e - k_u s_1 + k_{u0}\chi_u \\ \tau_{r0} = -\hat{\boldsymbol{\theta}}_r^T \boldsymbol{\xi}_1(\boldsymbol{v}) - c_2\dot{\psi}_e + \ddot{\psi}_d - \hat{V}_r - k_3 sgn(s_2) \\ \qquad - k_r s_2 - k_\psi \psi_e + k_{r0}\chi_r \end{cases} \tag{39}$$

The sign function will cause the system input chattering and it is not conducive to the stability of the system. So in order to address this issue, FLS is introduced to approximate the sign function. The equation set (39) can be rewritten as

$$\begin{cases} \tau_{u0} = -\hat{\boldsymbol{\theta}}_u^T \boldsymbol{\xi}_1(\boldsymbol{v}) + \dot{u}_d - \hat{V}_u - \hat{h}_1 - c_1 u_e - k_u s_1 \\ \qquad + k_{u0}\chi_u \\ \tau_{r0} = -\hat{\boldsymbol{\theta}}_r^T \boldsymbol{\xi}_1(\boldsymbol{v}) - c_2\dot{\psi}_e + \ddot{\psi}_d - \hat{V}_r - \hat{h}_2 - k_r s_2 \\ \qquad - k_\psi \psi_e + k_{r0}\chi_r \end{cases} \tag{40}$$

where $\hat{h}_1 = \hat{\theta}_{h1}^T \xi_2(s_1)$ represents the approximation to $k_1 sgn(s_1)$, and $\hat{h}_2 = \hat{\theta}_{h2}^T \xi_2(s_2)$ denotes the approximation to $k_3 sgn(s_2)$. The input of FLS are s_1 and s_2.

Remark 7: In practices, the ocean currents velocity and other disturbances are all bounded [30], therefore, Assumption 5 is reasonable. It is explained in [44] that $\boldsymbol{\vartheta}_u^T(\psi, r)\boldsymbol{V}_{xy}$ and $\boldsymbol{\vartheta}_r^T(u, v, r, \psi)\boldsymbol{V}_{xy}$ are slow time-varying and they are all bounded so that $V_u \le V_{u\max}$ and $V_r \le V_{r\max}$. Thus, it is feasible to utilize the adaptive method to estimate V_u and V_r. In this paper, we only estimate V_u and V_r in order to facilitate the design of the controller, and we can easily accurately calculate the ocean current velocities if the dynamics of USV model are all known. Besides, the purpose we deal with the ocean currents and USV uncertainties separately is to lay the groundwork for future research.

The update laws of FLS and adaptive laws are designed as

$$\begin{cases} \dot{\hat{\boldsymbol{\theta}}}_u = \gamma_1(s_1\boldsymbol{\xi}_1(\boldsymbol{v}) - \varphi_u\hat{\boldsymbol{\theta}}_u) \\ \dot{\hat{\boldsymbol{\theta}}}_r = \gamma_2(s_2\boldsymbol{\xi}_1(\boldsymbol{v}) - \varphi_r\hat{\boldsymbol{\theta}}_r) \\ \dot{\hat{V}}_u = \Gamma_1(s_1 - \vartheta_u\hat{V}_u) \\ \dot{\hat{V}}_r = \Gamma_2(s_2 - \vartheta_r\hat{V}_r) \\ \dot{\hat{\theta}}_{h1} = \rho_1(s_1\xi_2(s_1) - q_u\hat{\theta}_{h1}) \\ \dot{\hat{\theta}}_{h2} = \rho_2(s_2\xi_2(s_2) - q_r\hat{\theta}_{h2}) \end{cases} \tag{41}$$

where $\gamma_1, \gamma_2, \Gamma_1, \Gamma_2, \rho_1, \rho_2, \varphi_u, \varphi_r, \vartheta_u, \vartheta_r, q_u$ and q_r are positive parameters.

Theorem 3: The error signals of USV pathing following control system is SGUUB with the control laws (40), the adaptive laws (41), and tunning the positive parameters $c_1, c_2, k_{\chi u}, k_{\chi r}, \kappa_u, \kappa_r, \gamma_1, \gamma_2, \varphi_u, \varphi_r, \vartheta_u, \vartheta_r, \Gamma_1, \Gamma_2, \rho_1, \rho_2, q_u$ and q_r.

Proof: When $|\chi_i| \ge \chi_p (i = u, r)$, assign the following Lyapunov function

$$V_c = \frac{1}{2}s_1^2 + \frac{1}{2}\varphi_e^2 + \frac{1}{2}s_2^2 + \frac{1}{2\gamma_1}\tilde{\boldsymbol{\theta}}_u^T\tilde{\boldsymbol{\theta}}_u + \frac{1}{2\gamma_2}\tilde{\boldsymbol{\theta}}_r^T\tilde{\boldsymbol{\theta}}_r + \frac{1}{2\Gamma_1}\tilde{V}_u^2 + \frac{1}{2\Gamma_2}\tilde{V}_r^2 + \frac{1}{2\rho_1}\tilde{\theta}_{h1}^T\tilde{\theta}_{h1} + \frac{1}{2\rho_2}\tilde{\theta}_{h2}^T\tilde{\theta}_{h2} + \frac{1}{2}\chi_u^2 + \frac{1}{2}\chi_r^2 \tag{42}$$

The derivative of V_c along (35), (37), (38) (40) and (41) gives

$$\begin{aligned} \dot{V}_c = {} & s_1\Big(\tilde{\boldsymbol{\theta}}_u^T\boldsymbol{\xi}_1(\boldsymbol{v}) + \varepsilon_u + \tilde{V}_u - k_u s_1 - \hat{\theta}_{h1}^T\xi_2(s_1) \\ & + \theta_{h1}^T\xi_2(s_1) - \theta_{h1}^T\xi_2(s_1) + d_u + k_{u0}\chi_u + \Delta\tau_u\Big) \\ & - k_\psi c_2\psi_e^2 + k_\psi\psi_e s_2 + s_2\Big(\tilde{\boldsymbol{\theta}}_r^T\boldsymbol{\xi}_1(\boldsymbol{v}) + \varepsilon_r + \tilde{V}_r \\ & - k_r s_2 - k_\psi\psi_e + \hat{\theta}_{h2}^T\xi_2(s_2) + \theta_{h2}^T\xi_2(s_2) \\ & - \theta_{h2}^T\xi_2(s_2) + d_r + k_{r0}\chi_r + \Delta\tau_r\Big) - \frac{1}{\gamma_1}\tilde{\boldsymbol{\theta}}_u^T\dot{\hat{\boldsymbol{\theta}}}_u \\ & - \frac{1}{\gamma_2}\tilde{\boldsymbol{\theta}}_r^T\dot{\hat{\boldsymbol{\theta}}}_r - \frac{1}{\Gamma_1}\tilde{V}_u\dot{\hat{V}}_u - \frac{1}{\Gamma_2}\tilde{V}_r\dot{\hat{V}}_r - \frac{1}{\rho_1}\tilde{\theta}_{h1}^T\dot{\hat{\theta}}_{h1} \\ & - \frac{1}{\rho_2}\tilde{\theta}_{h2}^T\dot{\hat{\theta}}_{h2} + \chi_u\dot{\chi}_u + \chi_r\dot{\chi}_r \end{aligned} \tag{43}$$

According to Lemma 1, substituting (41) into (43) yields

$$\begin{aligned} \dot{V}_c \le {} & -\left(k_u - 1 - \frac{1}{2}k_{u0}\right)s_1^2 - \left(k_r - 1 - \frac{1}{2}k_{r0}\right)s_2^2 \\ & - \left(k_{\chi u} - \frac{k_{u0}}{2} - \frac{1}{2}\right)\chi_u^2 - \left(k_{\chi r} - \frac{k_{r0}}{2} - \frac{1}{2}\right)\chi_r^2 \\ & - k_\psi c_2\psi_e^2 - \frac{\varphi_u}{2}\tilde{\boldsymbol{\theta}}_u^T\tilde{\boldsymbol{\theta}}_u - \frac{\varphi_r}{2}\tilde{\boldsymbol{\theta}}_r^T\tilde{\boldsymbol{\theta}}_r - \frac{\vartheta_u}{2}\tilde{V}_u^2 - \frac{\vartheta_r}{2}\tilde{V}_r^2 \\ & - \frac{q_u}{2}\tilde{\theta}_{h1}^T\tilde{\theta}_{h1} - \frac{q_r}{2}\tilde{\theta}_{h2}^T\tilde{\theta}_{h2} + \frac{1}{2}\left(\varepsilon_u^2 + \varepsilon_r^2 + \varepsilon_{h1}^2 + \varepsilon_{h2}^2\right) \\ & + \frac{\varphi_u}{2}\theta_{u\max}^2 + \frac{\varphi_r}{2}\theta_{r\max}^2 + \frac{\vartheta_u}{2}V_{u\max}^2 \\ & + \frac{\vartheta_r}{2}V_{r\max}^2 + \frac{q_u}{2}\theta_{h1\max}^2 + \frac{q_r}{2}\theta_{h2\max}^2 \\ & + s_1 d_u - k_1|s_1| + s_2 d_r - k_3|s_2| \\ \le {} & -2\mu_{3a}V_c + C_{3a} \end{aligned} \tag{44}$$

where $\varepsilon_u, \varepsilon_r, \varepsilon_{h1}$ and ε_{h2} are the approximation error of $g_u, g_r, k_1 sgn(s_1)$ and $k_3 sgn(s_2)$. $\mu_{3a} = \min\{k_u - 1 - \frac{1}{2}k_{u0}, k_r - 1 - \frac{1}{2}k_{r0}, k_{\chi u} - \frac{k_{u0}}{2} - \frac{1}{2}, k_{\chi r} - \frac{k_{r0}}{2} - \frac{1}{2}, k_\psi c_2, \frac{\varphi_u}{2}\gamma_1, \frac{\varphi_r}{2}\gamma_2, \frac{\vartheta_u}{2}\Gamma_1, \frac{\vartheta_r}{2}\Gamma_2, \frac{q_u}{2}\rho_1, \frac{q_r}{2}\rho_2\} > 0$, and $C_{3a} = \frac{1}{2}(\varepsilon_u^2 + \varepsilon_r^2 + \varepsilon_{h1}^2 + \varepsilon_{h2}^2) + \frac{\varphi_u}{2}\theta_{u\max}^2 + \frac{\varphi_r}{2}\theta_{r\max}^2 + \frac{\vartheta_u}{2}V_{u\max}^2 + \frac{\vartheta_r}{2}V_{r\max}^2 + \frac{q_u}{2}\theta_{h1\max}^2 + \frac{q_r}{2}\theta_{h2\max}^2$

When $|\chi_i| < \chi_p (i = u, r)$, we don't have to analyse the boundness of χ_i, the Lyapunov function can become

$$V_c = \frac{1}{2}s_1^2 + \frac{1}{2}\varphi_e^2 + \frac{1}{2}s_2^2 + \frac{1}{2\gamma_1}\tilde{\boldsymbol{\theta}}_u^T\tilde{\boldsymbol{\theta}}_u + \frac{1}{2\gamma_2}\tilde{\boldsymbol{\theta}}_r^T\tilde{\boldsymbol{\theta}}_r + \frac{1}{2\Gamma_1}\tilde{V}_u^2 + \frac{1}{2\Gamma_2}\tilde{V}_r^2 + \frac{1}{2\rho_1}\tilde{\theta}_{h1}^T\tilde{\theta}_{h1} + \frac{1}{2\rho_2}\tilde{\theta}_{h2}^T\tilde{\theta}_{h2} \tag{45}$$

Differentiating V_c gives

$$\begin{aligned} \dot{V}_c = {} & s_1\Big(\tilde{\boldsymbol{\theta}}_u^T\boldsymbol{\xi}_1(\boldsymbol{v}) + \varepsilon_u + \tilde{V}_u - k_u s_1 - \hat{\theta}_{h1}^T\xi_2(s_1) \\ & + \theta_{h1}^T\xi_2(s_1) - \theta_{h1}^T\xi_2(s_1) + d_u + k_{u0}\chi_u + \Delta\tau_u\Big) \\ & - k_\psi c_2\psi_e^2 + k_\psi\psi_e s_2 + s_2\Big(\tilde{\boldsymbol{\theta}}_r^T\boldsymbol{\xi}_1(\boldsymbol{v}) + \varepsilon_r + \tilde{V}_r \\ & - k_r s_2 - k_\psi\psi_e + \hat{\theta}_{h2}^T\xi_2(s_2) + \theta_{h2}^T\xi_2(s_2) \\ & - \theta_{h2}^T\xi_2(s_2) + d_r + k_{r0}\chi_r + \Delta\tau_r\Big) - \frac{1}{\gamma_1}\tilde{\theta}_u^T\dot{\hat{\theta}}_u \\ & - \frac{1}{\gamma_2}\tilde{\theta}_r^T\dot{\hat{\theta}}_r - \frac{1}{\Gamma_1}\tilde{V}_u\dot{\hat{V}}_u - \frac{1}{\Gamma_2}\tilde{V}_r\dot{\hat{V}}_r - \frac{1}{\rho_1}\tilde{\theta}_{h1}^T\dot{\hat{\theta}}_{h1} \\ & - \frac{1}{\rho_2}\tilde{\theta}_{h2}^T\dot{\hat{\theta}}_{h2} \end{aligned}$$

$$\leq -\left(k_u - \frac{3}{2} - \frac{1}{2}k_{u0}\right)s_1^2 - \left(k_r - \frac{3}{2} - \frac{1}{2}k_{r0}\right)s_2^2 - \left(k_{\chi u} - \frac{k_{u0}}{2} - \frac{1}{2}\right)\chi_u^2 - \left(k_{\chi r} - \frac{k_{r0}}{2} - \frac{1}{2}\right)\chi_r^2 - k_\psi c_2\psi_e^2 - \frac{\varphi_u}{2}\tilde{\boldsymbol{\theta}}_u^T\tilde{\boldsymbol{\theta}}_u - \frac{\varphi_r}{2}\tilde{\boldsymbol{\theta}}_r^T\tilde{\boldsymbol{\theta}}_r - \frac{\vartheta_u}{2}\tilde{V}_u^2 - \frac{\vartheta_r}{2}\tilde{V}_r^2 - \frac{\rho_u}{2}\tilde{\theta}_{h1}^T\tilde{\theta}_{h1} - \frac{\rho_r}{2}\tilde{\theta}_{h2}^T\tilde{\theta}_{h2} + \frac{1}{2}\left(\varepsilon_u^2 + \varepsilon_r^2 + \varepsilon_{h1}^2 + \varepsilon_{h2}^2\right) + \frac{\varphi_u}{2}\theta_{u\max}^2 + \frac{\varphi_r}{2}\theta_{r\max}^2 + \frac{\vartheta_u}{2}V_{u\max}^2 + \frac{\vartheta_r}{2}V_{r\max}^2 + \frac{q_u}{2}\theta_{h1\max}^2 + \frac{q_r}{2}\theta_{h2\max}^2 + s_1d_u - k_1|s_1| + s_2d_r - k_3|s_2| + \frac{1}{2}\Delta\tau_u^2 + \frac{1}{2}\Delta\tau_r^2$$
$$\leq -2\mu_{3b}V_c + C_{3b} \tag{46}$$

where $\mu_{3b} = \min\{k_u - \frac{3}{2} - \frac{1}{2}k_{u0}, k_r - \frac{3}{2} - \frac{1}{2}k_{r0}, k_{\chi u} - \frac{k_{u0}}{2} - \frac{1}{2}, k_{\chi r} - \frac{k_{r0}}{2} - \frac{1}{2}, k_\psi c_2, \frac{\varphi_u}{2}\gamma_1, \frac{\varphi_r}{2}\gamma_2, \frac{\vartheta_u}{2}\Gamma_1, \frac{\vartheta_r}{2}\Gamma_2, \frac{q_u}{2}\rho_1, \frac{q_r}{2}\rho_2\} > 0$, and $C_{3b} = \frac{1}{2}(\varepsilon_u^2 + \varepsilon_r^2 + \varepsilon_{h1}^2 + \varepsilon_{h2}^2) + \frac{\varphi_u}{2}\theta_{u\max}^2 + \frac{\varphi_r}{2}\theta_{r\max}^2 + \frac{\vartheta_u}{2}V_{u\max}^2 + \frac{\vartheta_r}{2}V_{r\max}^2 + \frac{q_u}{2}\theta_{h1\max}^2 + \frac{q_r}{2}\theta_{h2\max}^2 + \frac{1}{2}\Delta\tau_u^2 + \frac{1}{2}\Delta\tau_r^2$.

When $|\chi_u| \geq \chi_p, \chi_r < \chi_p$ or $|\chi_r| \geq \chi_p, \chi_u < \chi_p$, the analysis is similar to the above, so no more expatiation here. We can obtain $V_c \leq -2\mu_{3c}V_c + C_{3c}$ and $V_c \leq -2\mu_{3d}V_c + C_{3d}$.

Remark 8: When $\chi_i \geq \chi_p (i = u, r)$, there exists input saturation. If $\chi_i < \chi_p$ and $\dot{\chi}_i = 0$, it means that there is no saturation, and that gives $\Delta\tau_i = 0$. Therefore, C_{3b}, C_{3c} and C_{3d} are all bounded.

Thus, $\dot{V}_c$ is strictly negative outside the range $\varpi_3 = \{V_c \leq \frac{C_3}{2\mu_3}\}$ and that gives

$$V_c \leq (V_c(0) - \frac{C_3}{2\mu_3})e^{-2\mu_3 t} + \frac{C_3}{2\mu_3} \tag{47}$$

where $\mu_3 = \min\{\mu_{3a}, \mu_{3b}, \mu_{3c}, \mu_{3d}\}$ and $C_3 = \max\{C_{3a}, C_{3b}, C_{3c}, C_{3d}\}$. it follows that all the velocity errors and approximation errors are SGUUB, the control subsystem is stable.

There is no control input on sway direction due to the USV in this paper is underactuated, the boundness of the sway velocity will be proved later.

V. CLOSED-LOOP SYSTEM STABILITY ANALYSIS

Theorem 4: Consider the USV model (5), the errors are defined as $\boldsymbol{\zeta}_e = [\boldsymbol{a}_e, \boldsymbol{b}_e, \boldsymbol{c}_e]^T$, where $\boldsymbol{a}_e = [x_e, y_e]^T$, $\boldsymbol{b}_e = [s_1, \psi_e, s_2]^T$ and $\boldsymbol{c}_e = [\tilde{\boldsymbol{\theta}}_u, \tilde{\boldsymbol{\theta}}_r, \tilde{V}_u, \tilde{V}_r, \tilde{\theta}_{h1}, \tilde{\theta}_{h2}]^T$, in the presence of unknown dynamics and disturbances, and suppose that Assumptions 1-4 are satisfied. If the guidance law is obtained by (20), the auxiliary systems are presented by (37) and (38), the controllers are designed by (40), and the weights of FLS and ocean current terms are updated by (41), then the following holds:

(1) The calculated value of time-varying sideslip angle is bounded.

(2) The closed-loop system that contains guidance and execution is SGUUB. The position tracking errors (x_e, y_e), the velocity and attitude tracking errors (s_1, ψ_e, s_2) and the estimation errors $(\tilde{\boldsymbol{\theta}}_u, \tilde{\boldsymbol{\theta}}_r, \tilde{V}_u, \tilde{V}_r, \tilde{\theta}_{h1}, \tilde{\theta}_{h2})$ converge to the domain near the origin.

(3) The sway velocity is uniformly ultimately bounded.

Proof: (1) Seeing that $\tilde{g}$ is bounded from Theorem 1, and there is little difference between ψ_d and α_p as we can find from Figure 1 and this results in that the value of $\cos(\psi_d - \alpha_p)$ is in the vicinity of 1. Thus, $\tilde{\beta} = \tilde{g}/U\cos(\psi_d - \alpha_p)$ is bounded. For $\hat{\beta} = \tilde{\beta} + \beta$, we assume that the sideslip is small in this paper, so we can conclude that the estimation of sideslip angle is always bounded.

(2) Assign the complete Lyapunov function $V = V_2 + V_c$. The derivative of V satisfies $\dot{V} \leq \mu_2 V_2 + \mu_3 V_c + C_2 + C_3 \leq \mu V + C$, where $\mu = \min\{\mu_2, \mu_3\}$ and $C = C_2 + C_3$ such that

$$V \leq (V(0) - \frac{C}{2\mu})e^{-2\mu t} + \frac{C}{2\mu} \tag{48}$$

It follows that the tracking errors $\boldsymbol{a}_e, \boldsymbol{b}_e$ and the estimation error $\boldsymbol{c}_e$ are all bounded. Thus, the closed-loop path following system is SGUUB.

(3) There is no lateral thrust of USV, for its dynamic, assign a Lyapunov function $V_v = \frac{1}{2}V_v^2$, the derivative of V_v can be expressed as

$$\begin{aligned}\dot{V}_v &= A(u_r, u_c)vr + B(u_r)(v - v_c)v + vd_v \\ &= B(u_r)v^2 + A(u_r, u_c)vr - B(u_r)v_cv + vd_v \\ &\leq B(u_r)v^2 + |A(u_r, u_c)v - B(u_r)v_c + d_v||v|\end{aligned} \tag{49}$$

Since $B(u_r), A(u_r, u_c), v_c, d_v$ and r are all bounded and $B(u_r) < 0$ [45], the sway velocity which is not controlled directly is uniformly ultimately bounded according to Chapter 4 of [46].

That concludes the proof.

VI. SIMULATION STUDIES

In order to enhance the path following performance, the adjustment of control parameters seems particularly important. For the observer (15), η_1 to η_5 and τ should satisfy the conditions mentioned in the proof of *Theorem 1*. Besides, a bigger τ leads more smooth of y_e, but it will cause the magnifying of sideslip angle estimation. k is the control parameter of virtual velocity, and the size of k determines the speed of reference path as mentioned in *Remark 5*, a larger k will make the reference path go faster, meanwhile, the oscillation of x_e will appear on the system. For the velocity and attitude controller, it is obviously seen that a larger μ_3 and a smaller C_3 results in smaller error signals, and this can obtained by selecting larger $k_u, k_r, k_{\chi u}, k_{\chi r}, k_\psi, c_2, \gamma_1, \gamma_2, \Gamma_1, \Gamma_2, \rho_1, \rho_2$ and smaller $k_{u0}, k_{r0}, \varphi_u, \varphi_r, \vartheta_u, \vartheta_r, q_u, q_r$, in which $\gamma_1, \gamma_2, \rho_1$ and ρ_2 can affect the learning speed of FLS and the ability of robust term to compensate error. Nevertheless, if k_{u0} and k_{r0} are too small, the compensation effect of the auxiliary system is not so good.

In order to verify the availability of the proposed filter-extended state observer based guidance law with adaptive fuzzy control (FEAFC) scheme, we conduct some

simulation studies in this section with the USV whose parameters can be found in [45]. The maximum magnitude of the surge force and yaw moments are 2 N and 1.5 Nm, respectively [47]. The parameters of path following control system are shown in Table 2. The ocean currents are given as $V_x = 0.05$m/s, $V_y = 0.03$m/s and the other disturbances assumed as $[d_u, d_v, d_r]^T = [0.3\sin(0.1t), 0.2\sin(0.1t), 0.2\sin(0.1t)\ ]^T$. To highlight the superiority of the proposed scheme, a comparison between FEAFC and extended state observer based guidance law with adaptive fuzzy control (EAFC) method is conducted, and we also consider a comparison between variable look-ahead distance (VLD) and fixed look-ahead distance (FLD).

TABLE 2. Control parameters of USV simulation.

Notation	Value	Notation	Value	Notation	Value
τ	0.1	k_u	5	φ_u	0.2
η_1	5	k_r	3	φ_r	0.3
η_2	0.1	k_ψ	1	Γ_1	5
η_3	5	$k_{\chi u}$	1.5	Γ_2	10
η_4	0.1	$k_{\chi r}$	2.5	ϑ_u	0.3
η_5	3	κ_u	1	ϑ_r	0.3
k	6	κ_r	1	ρ_1	5
c_1	3	k_{u0}	5	ρ_2	5
c_2	3	k_{r0}	2	q_u	0.1
α	0.8	γ_1	10	q_r	0.2
δ	0.6	γ_2	30	χ_p	0.001

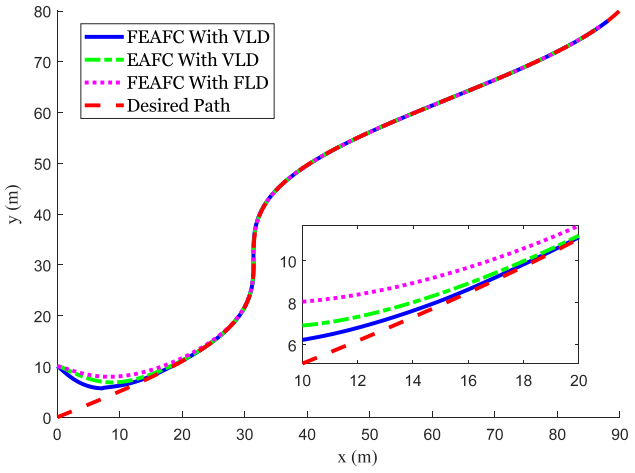

FIGURE 3. Path following results.

The initial values of $\theta_u, \theta_r, \theta_{h1}$ and θ_{h2} are given in (0, 1) at random. The desired path is parameterized by

$$\begin{cases} x_p(\omega) = 10\sin(0.1\omega) + \omega \\ y_p = \omega \end{cases} \tag{50}$$

The desired surge velocity are given as 0.5m/s, and the initial conditions of USV are set by $[x(0), y(0), u(0), v(0), r(0), \psi(0)]^T = [0, 10, 0, 0.01, 0, 0]^T$.

The simulation results are demonstrated in Figs. 3-13. Figs. 3-4 illustrate that FEAFC with VLD performs best

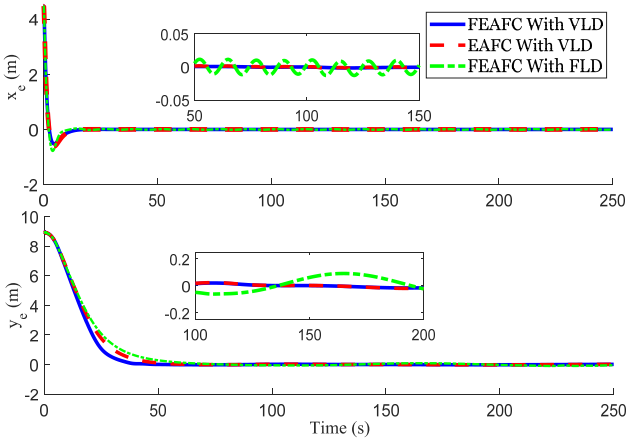

FIGURE 4. Position errors of path following.

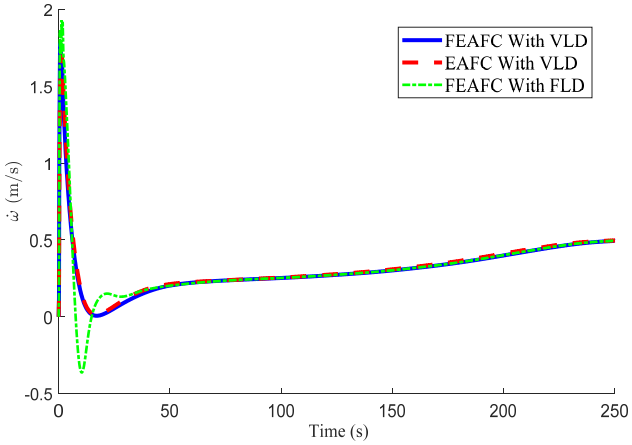

FIGURE 5. The update law of path variable.

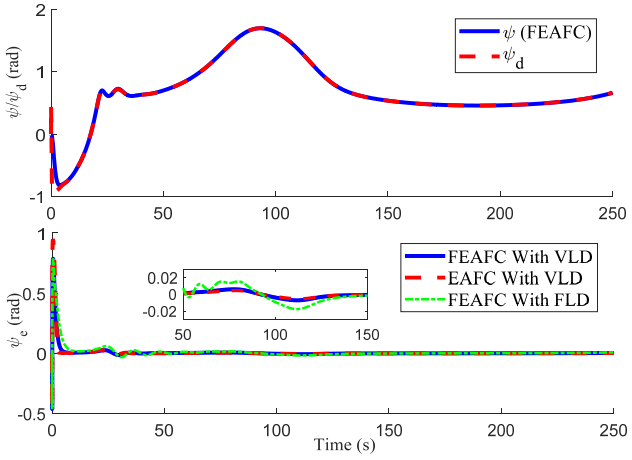

FIGURE 6. The attitude performance.

because it converges to the desired path fastest, besides, it has the lowest chattering in the stable-state of along and cross tracking errors. The update law of parametric path and heading angle performances are shown in Figs. 5-6, $\dot{\omega}$ represents the speed of the reference path and the stability of VLD schemes preform better. The FLD scheme exhibits obvious fluctuating behaviour at the stable-state in Fig 6. The

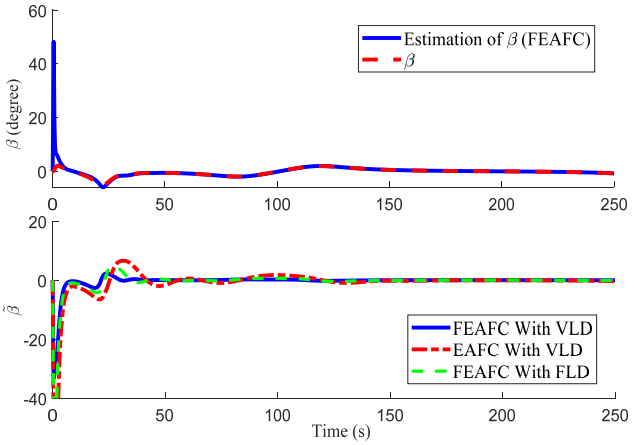

FIGURE 7. The estimation error of β.

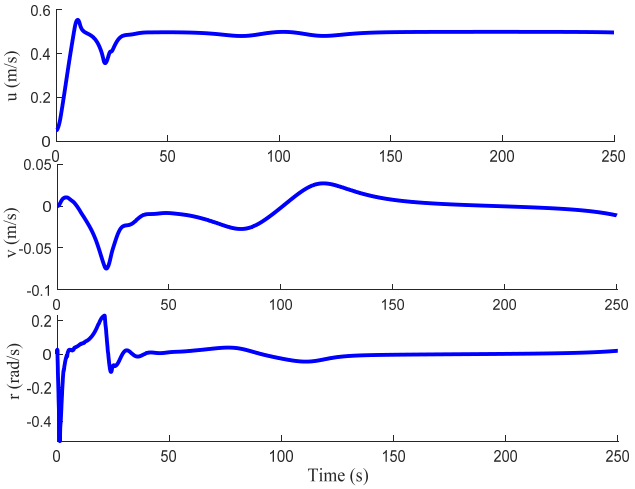

FIGURE 8. Velocities and yaw rate performances.

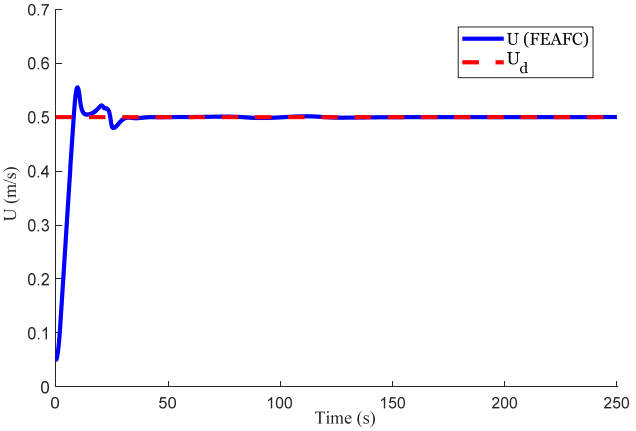

FIGURE 9. Resultant velocity and desired velocity.

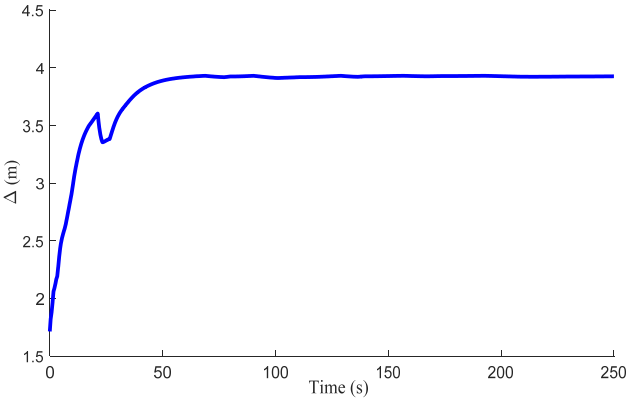

FIGURE 10. Look-ahead distance.

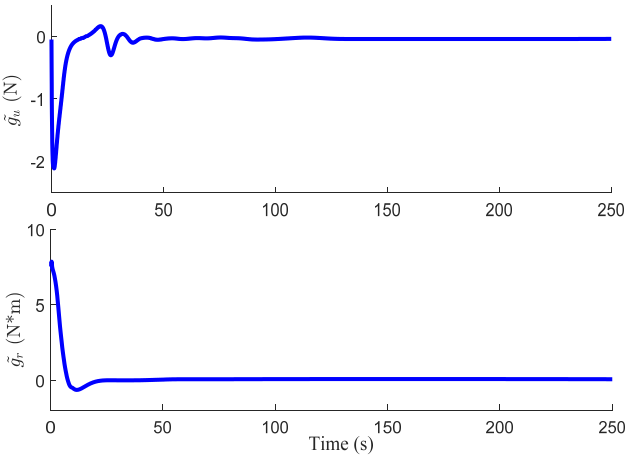

FIGURE 11. The approximation errors of unknown dynamics.

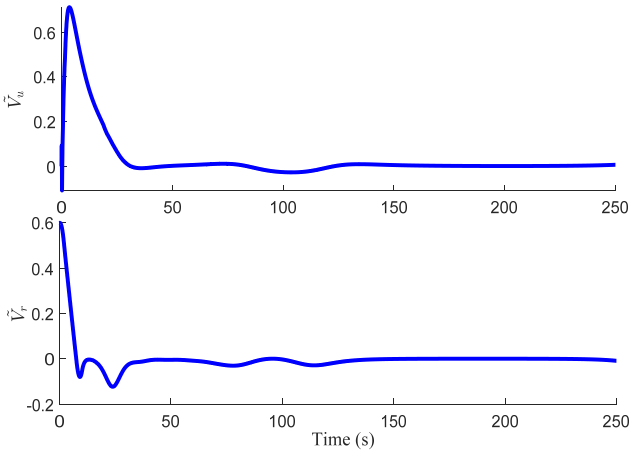

FIGURE 12. The estimation errors of V_u and V_r.

estimation of sideslip is shown in Fig. 7, from which we can find that FEAFC scheme has a better estimation effect. Then, Figs. 8-9 describe the system state, that is the velocities and yaw rate, which illustrate that the USV state can follow the desired state rapidly and accurately. In Figs. 11-12, with the influence of the robust FLS and adaptive method, the approximation errors of uncertainties and estimation errors of ocean current disturbances can be convergent to zero. We can see from Fig. 12 that there are some oscillations in the steady state since V_u and V_r are not strict time-invariant and the adaptive method has limited capacity to deal with time-varying signals. The inputs are in the specified region which can be found in Fig. 13, it is indicated that the problem of actuator saturation is efficaciously solved by auxiliary

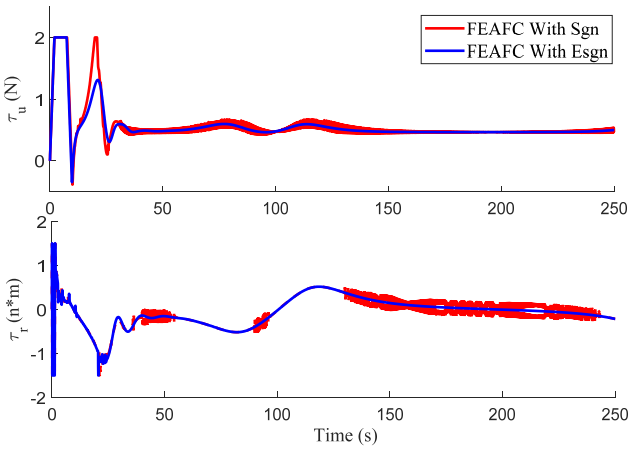

FIGURE 13. The control laws.

system. Besides, a comparison is conducted between the control law with sign function (sgn) and with the estimation of sign function (esgn) by FLS. We can find the control force and moment with esgn are smooth and realistic. It is worth mentioning that the input signals will destroy actuators seriously without and anti-fluctuation.

VII. CONCLUSION

In this paper, an FEAFC scheme for path following of underactuated USV is proposed, in which FESO is served as estimating the time-varying sideslip angle, FLS is applied to approximate the unknown dynamics of USV and the sign functions contained in the input signals, and the ocean current disturbances are estimated by the adaptive method. Rigorous analysis demonstrates that all the tracking errors of the path following system are SGUUB. Finally, the simulation results indicate the correctness and superiority of presented FEAFC scheme. Besides, it should be pointed out that although the proposed scheme is designed for USV, it is also suitable for other vehicles, such as autonomous underwater vehicle (AUV).

This paper consider as many actual conditions that impact the system as possible, but there are still some problems that need to be investigated thoroughly, such as the hysteresis characteristics of actuator, the relationship between the rudder angle and yaw moment, *etc*. These problems will be researched in our future works.

APPENDIX

$$\vartheta_u(\psi, r) = \begin{bmatrix} \dfrac{d_{11}+2d_{11}^q u}{m_{11}}\cos(\psi) - \dfrac{m_{11}^A - m_{22}^A}{m_{11}}\sin(\psi) \\ \dfrac{d_{11}+2d_{11}^q u}{m_{11}}\sin(\psi) + \dfrac{m_{11}^A - m_{22}^A}{m_{11}}\cos(\psi) \\ -d_{11}^q\cos^2(\psi) \\ -d_{11}^q\sin^2(\psi) \\ -d_{11}^q\cos(\psi)\sin(\psi) \end{bmatrix}$$

$$\begin{cases} A(u_r, u_c) = \dfrac{1}{\Omega}[m_{33}(-d_{23} - m_{11}u_r - m_{11}^{RB}u_c) \\ \qquad + m_{23}d_{33} + m_{23}(m_{23}u_r + m_{23}^{RB}u_c + m_{22}^A u_c)] \\ B(u_r) = \dfrac{1}{\Omega}[-m_{33}d_{22} + m_{23}d_{32} + m_{23}(m_{22}^A - m_{11}^A u_r)] \\ C_r(u, v, r) = -\dfrac{m_{23}}{\Omega}(-m_{11}ur - d_{22}v - d_{23}r) \\ \qquad + \dfrac{m_{22}}{\Omega}[-(m_{22}v - m_{23}r)u + m_{11}uv \\ \qquad - d_{32}v - d_{33}r] \end{cases}$$

where $\Omega = m_{22}m_{33} - m_{23}^2 > 0$, $\boldsymbol{\vartheta}_r(u, v, r, \psi) = [\vartheta_{r1}, \vartheta_{r2}, \vartheta_{r3}, \vartheta_{r4}, \vartheta_{r5}]^T$,

$$\begin{cases} \begin{bmatrix} \vartheta_{r1} \\ \vartheta_{r2} \end{bmatrix} = \begin{bmatrix} \cos(\psi) & -\sin(\psi) \\ \sin(\psi) & \cos(\psi) \end{bmatrix} \begin{bmatrix} l_1 \\ l_2 \end{bmatrix} \\ \vartheta_{r3} = -\dfrac{m_{22}}{\Omega}(m_{11}^A - m_{22}^A)\sin(\psi)\cos(\psi) \\ \vartheta_{r4} = \dfrac{m_{22}}{\Omega}(m_{11}^A - m_{22}^A)\sin(\psi)\cos(\psi) \\ \vartheta_{r5} = \dfrac{m_{22}}{\Omega}(m_{11}^A - m_{22}^A)(1 - 2\sin^2(\psi)) \end{cases}$$

$$\begin{cases} l_1 = -\dfrac{m_{22}}{\Omega}[(m_{11}^A - m_{22}^A)v + (m_{23}^A - m_{22}^A)r] - \dfrac{m_{23}}{\Omega}m_{11}^A r \\ l_2 = \dfrac{m_{22}}{\Omega}[d_{32} - (m_{11}^A - m_{22}^A)u] - \dfrac{m_{23}}{\Omega}d_{22} \end{cases}$$

ACKNOWLEDGMENT

The authors would like to thank editor and reviewers for their valuable suggestions.

REFERENCES

[1] T. I. Fossen, K. Y. Pettersen, and R. Galeazzi, "Line-of-sight path following for Dubins paths with adaptive sideslip compensation of drift forces," *IEEE Trans. Control Syst. Technol.*, vol. 23, no. 2, pp. 820–827, Mar. 2015.

[2] G. Zhang and X. Zhang, "Concise robust adaptive path-following control of underactuated ships using DSC and MLP," *IEEE J. Ocean. Eng.*, vol. 39, no. 4, pp. 685–694, Oct. 2014.

[3] G. Zhu and J. Du, "Global robust adaptive trajectory tracking control for surface ships under input saturation," *IEEE J. Ocean. Eng.*, to be published.

[4] D. D. Mu, G. F. Wang, Y. S. Fan, Y. M. Bai, and Y. S. Zhao, "Path following for podded propulsion unmanned surface vehicle: Theory, simulation and experiment," *IEEJ Trans. Elect. Electron. Eng.*, vol. 13, no. 5, pp. 911–923, Mar. 2018.

[5] T. I. Fossen, *Handbook Marine Craft Hydrodynamics Motion Control*. New York, NY, USA: Wiley, 2011.

[6] A. J. Healey and D. Lienard, "Multivariable sliding mode control for autonomous diving and steering of unmanned underwater vehicles," *IEEE J. Ocean. Eng.*, vol. 18, no. 3, pp. 327–339, Jul. 1993.

[7] S.-R. Oh and J. Sun, "Path following of underactuated marine surface vessels using line-of-sight based model predictive control," *Ocean Eng.*, vol. 37, nos. 2–3, pp. 289–295, Feb. 2010.

[8] E. Borhaug, A. Pavlov, and K. Y. Pettersen, "Integral LOS control for path following of underactuated marine surface vessels in the presence of constant ocean currents," in *Proc. IEEE Conf. Decision Control*, Cancun, Mexico, Dec. 2008, pp. 4984–4991.

[9] A. M. Lekkas and T. I. Fossen, "Integral LOS path following for curved paths based on a monotone cubic Hermite spline parametrization," *IEEE Trans. Control Syst. Technol.*, vol. 22, no. 6, pp. 2287–2301, Nov. 2014.

[10] T. I. Fossen and A. M. Lekkas, "Direct and indirect adaptive integral line-of-sight path-following controllers for marine craft exposed to ocean currents," *Int. J. Adapt. Control Signal Process.*, vol. 31, no. 4, pp. 445–463, Apr. 2017.

[11] W. Caharija, K. Y. Pettersen, M. Bibuli, P. Calado, E. Zereik, J. Braga, J. T. Gravdahl, A. J. Sørensen, M. Milovanovic, and G. Bruzzone, "Integral line-of-sight guidance and control of underactuated marine vehicles: Theory, simulations, and experiments," *IEEE Trans. Control Syst. Technol.*, vol. 24, no. 5, pp. 1623–1642, Sep. 2016.

[12] D. M. Bevly, R. Sheridan, and J. C. Gerdes, "Integrating INS sensors with GPS velocity measurements for continuous estimation of vehicle sideslip and tire cornering stiffness," in *Proc. Amer. Control Conf.*, Arlington, VA, USA, Jun. 2001, pp. 483–493.
[13] L. Liu, D. Wang, and Z. Peng, "ESO-based line-of-sight guidance law for path following of underactuated marine surface vehicles with exact sideslip compensation," *IEEE J. Ocean. Eng.*, vol. 42, no. 2, pp. 477–487, Apr. 2017.
[14] L. Liu, D. Wang, Z. Peng, and H. Wang, "Predictor-based LOS guidance law for path following of underactuated marine surface vehicles with sideslip compensation," *Ocean Eng.*, vol. 124, pp. 340–348, Sep. 2016.
[15] N. Wang, Z. Sun, J. Yin, S.-F. Su, and S. Sharma, "Finite-time observer based guidance and control of underactuated surface vehicles with unknown sideslip angles and disturbances," *IEEE Access*, vol. 6, pp. 14059–14070, 2018.
[16] N. Wang, Z. Sun, Z. Zheng, and H. Zhao, "Finite-time sideslip observer-based adaptive fuzzy path-following control of underactuated marine vehicles with time-varying large sideslip," *Int. J. Fuzzy Syst.*, vol. 20, no. 5, pp. 1–12, Sep. 2017.
[17] B. Qiu, G. Wang, Y. Fan, D. Mu, and X. Sun, "Adaptive course control-based trajectory linearization control for uncertain unmanned surface vehicle under rudder saturation," *IEEE Access*, vol. 7, pp. 108768–108780, 2019.
[18] B. Qiu, G. Wang, and Y. Fan, "Robust course controller based trajectory linearization control for unmanned surface vehicle with input saturation," *Mech. Syst. Control.*, vol. 47, no. 4, pp. 187–193, 2019.
[19] R. Wang, S. Wang, Y. Wang, and C. Tang, "Path following for a biomimetic underwater vehicle based on ADRC," in *Proc. IEEE Int. Conf. Robot. Automat.*, May/Jun. 2017, pp. 3519–3524.
[20] B. Yi, L. Qiao, and W. Zhang, "Two-time scale path following of underactuated marine surface vessels: Design and stability analysis using singular perturbation methods," *Ocean Eng.*, vol. 124, pp. 287–297, Sep. 2016.
[21] R. Skjetne and T. I. Fossen, "Nonlinear maneuvering and control of ships," in *Proc. OCEANS MTS/IEEE Conf. Exhibit.*, Honolulu, HI, USA, Nov. 2001, pp. 1808–1815.
[22] K. D. Do and J. Pan, "State and output-feedback robust path-following controllers for underactuated ships using Serret-Frenet frame," *Ocean Eng.*, vol. 31, nos. 5–6, pp. 587–613, Apr. 2004.
[23] J.-H. Li, P.-M. Lee, B.-H. Jun, and Y.-K. Lim, "Point-to-point navigation of underactuated ships," *Automatica*, vol. 44, no. 12, pp. 3201–3205, Dec. 2008.
[24] Q. Zou, F. Wang, L. Zou, and Q. Zong, "Robust adaptive constrained backstepping flight controller design for re-entry reusable launch vehicle under input constraint," *Adv. Mech. Eng.*, vol. 7, no. 9, pp. 1–13, Sep. 2015.
[25] X. Xiang, C. Liu, H. Su, and Q. Zhang, "On decentralized adaptive full-order sliding mode control of multiple UAVs," *ISA Trans.*, vol. 71, pp. 196–205, Nov. 2017.
[26] S. C.-Y. Chung and C.-L. Lin, "A transformed Lure problem for sliding mode control and chattering reduction," *IEEE Trans. Autom. Control*, vol. 44, no. 3, pp. 563–568, Mar. 1999.
[27] W. C. Su, "Sliding mode with chattering reduction in sampled data systems," in *Proc. IEEE Conf. Decis. Control*, Dec. 1993, pp. 2452–2457.
[28] W. Ham, "Adaptive fuzzy sliding mode control of nonlinear system," *IEEE Trans. Fuzzy Syst.*, vol. 6, no. 2, pp. 315–321, May 1998.
[29] Y. Konno and H. Hashimoto, "Design of sliding mode dynamics in the frequency domain," *Adv. Robot.*, vol. 7, no. 6, pp. 587–598, Jan. 1992.
[30] N. Wang and M. J. Er, "Direct adaptive fuzzy tracking control of marine vehicles with fully unknown parametric dynamics and uncertainties," *IEEE Trans. Control Syst. Technol.*, vol. 24, no. 5, pp. 1845–1852, Sep. 2016.
[31] G. Zhu, J. Du, and Y. Kao, "Command filtered robust adaptive NN control for a class of uncertain strict-feedback nonlinear systems under input saturation," *J. Franklin Inst.*, vol. 355, no. 15, pp. 7548–7569, Oct. 2018.
[32] Y.-F. Gao, X.-M. Sun, C. Wen, and W. Wang, "Observer-based adaptive NN control for a class of uncertain nonlinear systems with nonsymmetric input saturation," *IEEE Trans. Neural Netw. Learn. Syst.*, vol. 28, no. 7, pp. 1520–1530, Jul. 2017.
[33] Z. Yan, M. Wang, and J. Xu, "Global adaptive neural network control of underactuated autonomous underwater vehicles with parametric modeling uncertainty," *Asian J. Control*, vol. 21, no. 3, pp. 1342–1354, May 2019.
[34] G. Grimm, J. Hatfield, I. Postlethwaite, A. R. Teel, M. C. Turner, and L. Zaccarian, "Antiwindup for stable linear systems with input saturation: An LMI-based synthesis," *IEEE Trans. Autom. Control*, vol. 48, no. 9, pp. 1509–1525, Sep. 2003.
[35] M. Chen, Q. Wu, C. Jiang, and B. Jiang, "Guaranteed transient performance based control with input saturation for near space vehicles," *Sci. China Inf. Sci.*, vol. 57, no. 5, pp. 1–12, May 2014.
[36] Y. Li, S. Tong, and T. Li, "Direct adaptive fuzzy backstepping control of uncertain nonlinear systems in the presence of input saturation," *Neural Comput. Appl.*, vol. 23, no. 5, pp. 1207–1216, Oct. 2013.
[37] A. Loría, *Advanced Topics in Control Systems Theory*. London, U.K.: Springer, 2005.
[38] S. Yu, X. Yu, B. Shirinzadeh, and Z. Man, "Continuous finite-time control for robotic manipulators with terminal sliding mode," *Automatica*, vol. 41, no. 11, pp. 1957–1964, Nov. 2005.
[39] Y. L. Yu, C. Guo, and H. M. Yu, "Finite-time predictor line-of-sight-based adaptive neural network path following for unmanned surface vessels with unknown dynamics and input saturation," *Int. J. Adv. Rob. Syst.*, vol. 15, no. 6, pp. 1–14, Nov. 2018.
[40] M. Krstic, I. Kanellakopoulos, and P. Kokotovic, *Nonlinear and Adaptive Control Design*. New York, NY, USA: Wiley, 1995, ch. 5, pp. 185–232.
[41] A. M. Lekkas and T. I. Fossen, "Integral LOS path following for curved paths based on a monotone cubic hermite spline parametrization," *IEEE Trans. Control Syst. Technol.*, vol. 22, no. 6, pp. 2287–2301, Nov. 2014.
[42] H. J. Wang, "A new sliding mode guidance law based on extended state observer," *J. Solid Rocket Technol.*, vol. 38, no. 5, pp. 622–627, Oct. 2015.
[43] M. Chen, S. S. Ge, and B. Ren, "Adaptive tracking control of uncertain MIMO nonlinear systems with input constraints," *Automatica*, vol. 47, no. 3, pp. 452–465, Mar. 2011.
[44] T. I. Fossen, S. Moe, K. Y. Pettersen, and J. T. Gravdahl, "Line-of-sight curved path following for underactuated USVs and AUVs in the horizontal plane under the influence of ocean currents," in *Proc. Mediterr. Conf. Control Autom.*, 2016, pp. 38–45.
[45] Z. W. Zheng and L. Sun, "Path following control for marine surface vessel with uncertainties and input saturation," *Neurocomputing*, vol. 177, pp. 158–167, Nov. 2015.
[46] H. K. Khalil, *Nonlinear System*. Upper Saddle River, NJ, USA: Prentice-Hall, 2002.
[47] E. Fredriksen and K. Y. Pettersen, "Global-exponential waypoint maneuvering of ships: Theory and experiments," *Automatica*, vol. 42, no. 4, pp. 677–687, Apr. 2006.

MINGCONG LI received the B.E. degree in electrical engineering and automation, in 2013, and the M.S. degree in control engineering from Dalian Maritime University, Dalian, China, in 2016, where he is currently pursuing the Ph.D. degree in control theory and control engineering.

His research interests include motion control of unmanned surface vehicle, robust control, and fuzzy neural systems.

CHEN GUO received the B.E. degree from the Department of Automatic Control, Chongqing University, Chongqing, China, in 1982, and the M.Sc. and Ph.D. degrees in marine engineering automation from Dalian Maritime University, Dalian, China, in 1985 and 1992, respectively.

He is currently a Professor with the School of Marine Electrical Engineering and the Institute Director of Ship Automation and Simulator. His research interests include intelligent control, advanced ship borne detection device, and marine system automation and simulation.

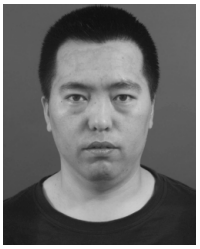

HAOMIAO YU received the B.E. and Ph.D. degrees in control theory and control engineering from Harbin Engineering University.

He is currently a Lecturer with Dalian Maritime University, Dalian, China. His research interests include nonlinear robust control systems and motion control of autonomous underwater vehicle.